

Supporting Information for: “*Ab Initio* Approach to Femtosecond Stimulated Raman Spectroscopy: Investigating Vibrational Modes Probed in Excited-State Relaxation of Quaterthiophenes”

Saswata Dasgupta and John M. Herbert*

July 9, 2020

*herbert@chemistry.ohio-state.edu

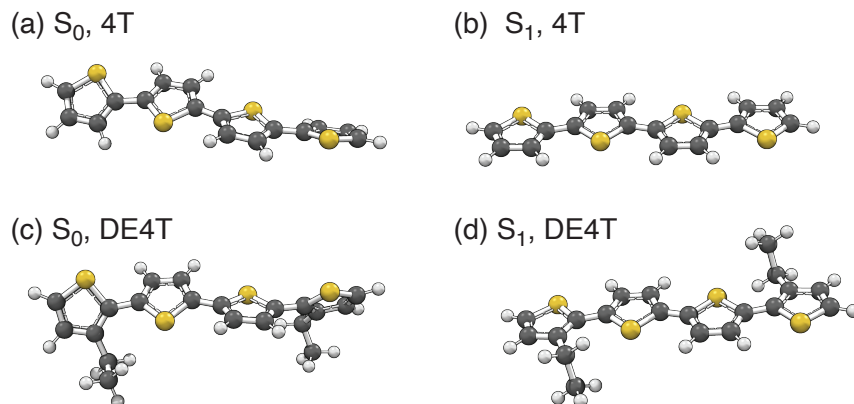


Figure S1: Fully-relaxed geometries of (a) the ground state of 4T, (b) the S_1 state of 4T, (c) the ground state of DE4T, and (d) the S_1 state of DE4T. For both molecules, the ground state exhibits a nonplanar thiophene backbone that is somewhat distorted with respect to the planar all-*trans* structure that represents the S_1 global-minimum geometry. Geometries were optimized at the CAM-B3LYP/6-31G* level of theory.

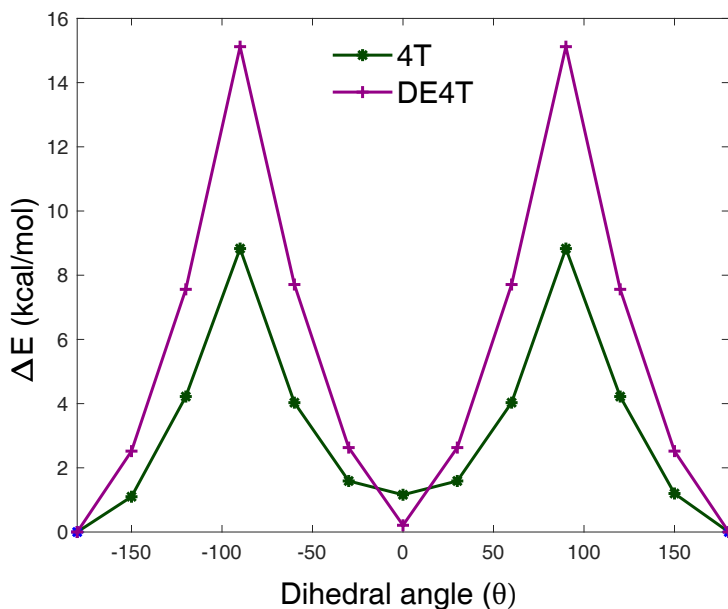


Figure S2: Potential energy scans for the S_1 state of 4T and DE4T along the torsional angle θ between the central thiophene rings. (This angle is depicted in Fig. 1.) Calculations were performed at the CAM-B3LYP/6-31G* level of theory, relaxing all degrees of freedom except for the interior dihedral angle θ . Values $\theta = \pm 180^\circ$ correspond to the all-*trans* minima depicted in Fig. S1, and $\theta = 0$ is the *trans-cis* structure.

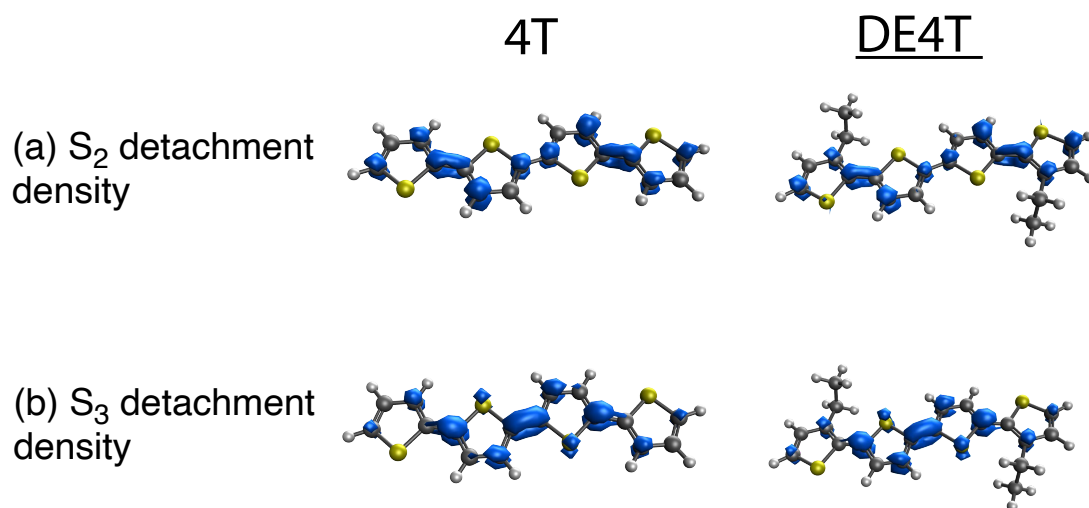


Figure S3: Attachment densities for (a) $S_0 \rightarrow S_2$ and (b) $S_0 \rightarrow S_3$ excitation of 4T and DE4T, computed at the at the S_1 minimum-energy geometry of either molecule using the CAM-B3LYP/6-31G* level of theory. These plots depict how the virtual MOs are occupied, relative to the ground-state electron configuration, upon vertical excitation. For both molecules, the S_2 state is characterized by incipient double-bond formation between the central and the peripheral thiophene rings whereas the S_3 state is characterized by double-bond formation between the central thiophene rings.

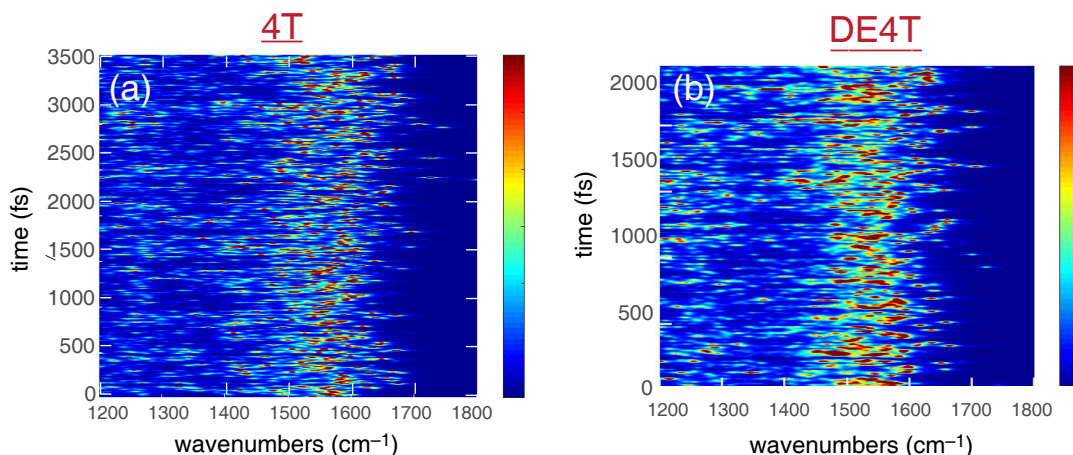


Figure S4: Time-evolving, instantaneous RR intensities corresponding to c excitation. These were computed from TD-DFT trajectories in the S_1 state of 4T (left) and DE4T (right). The color bar quantifies relative intensity enhancements and is therefore dimensionless. As compared to the RR intensities corresponding to $S_1 \rightarrow S_2$ excitation (Fig. 3), these spectra do not seem to describe the major features of the experimental spectra (Fig. 2). This, in addition to the vertical excitation energies (Table 1), leads us to conclude that resonant enhancement in the experiment occurs via $S_1 \rightarrow S_2$ excitation.

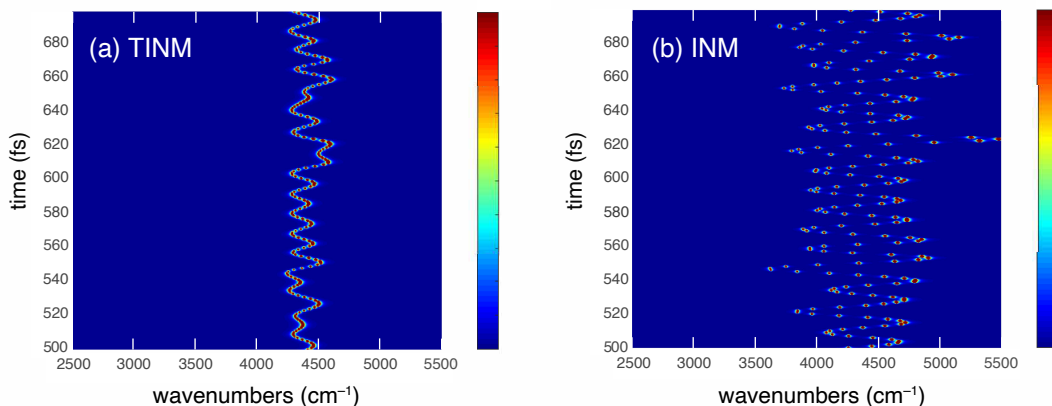


Figure S5: Ground state RR calculation ($S_0 \rightarrow S_1$) for H_2 , from *ai*MD trajectories at the B3LYP/6-31G* level, using (a) the time-averaged approach and (b) the standard INM approach. Although there can be no “resonance enhancement” (in the relative intensity, at least) for a molecule with only one vibrational mode, the intensity plotted here does include fluctuations in the excited-state gradient, which enters the intensity expression in Eq. (2) through the displacement Δ_k that is computed according to Eq. (9). The unitless colorbar defines the relative intensity of the spectra.

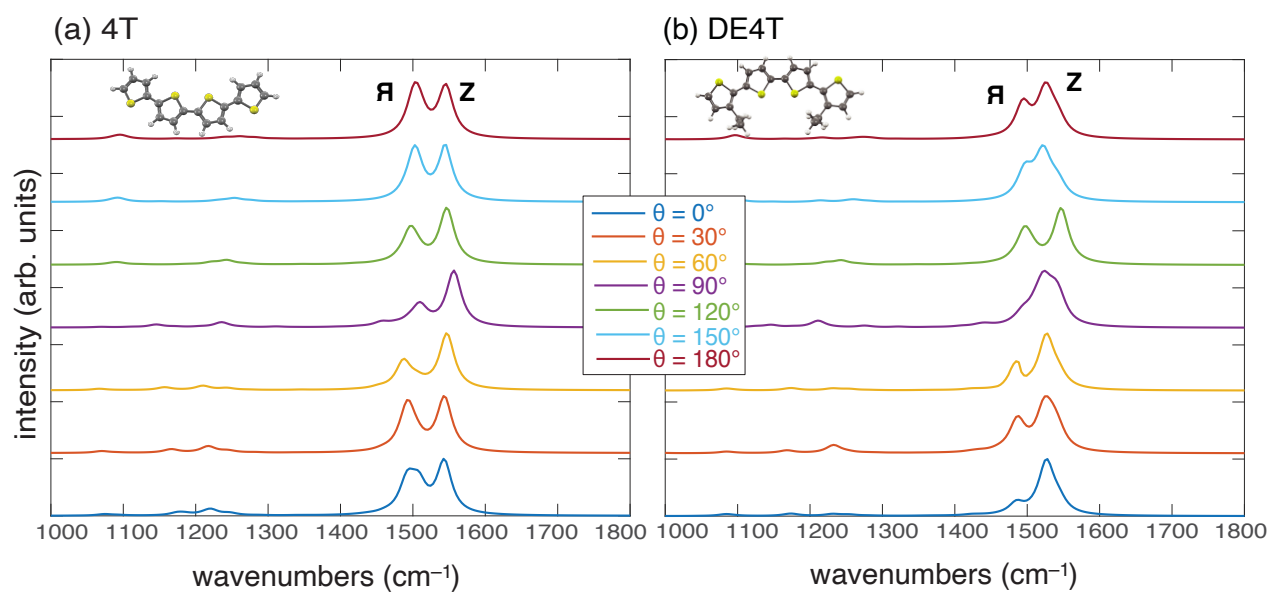


Figure S6: Stationary RR spectra ($S_1 \rightarrow S_2$ transition) for (a) 4T and (b) DE4T, computed at geometries optimized on the S_1 state. The fully-relaxed (minimum-energy S_1) geometry corresponds to the torsion angle $\theta = 180^\circ$, whereas other spectra are computed at constrained values of θ with all remaining coordinates relaxed on the S_1 state. (A subset of these spectra are depicted in Fig. 6.) Calculations were performed using TD-DFT at the CAM-B3LYP/6-31G* level.

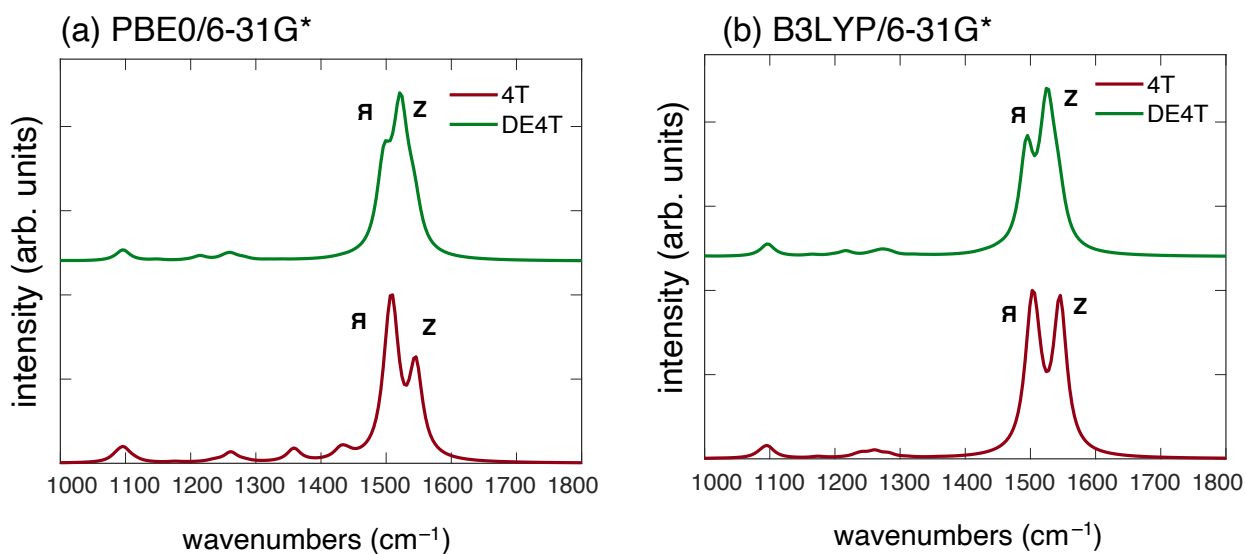


Figure S7: Stationary RR spectra ($S_1 \rightarrow S_2$ transition) for 4T and DE4T, computed at geometries optimized on the S_1 state, using TD-DFT at (a) the PBE0/6-31G* level, versus (b) the B3LYP/6-31G* level. Results are qualitatively similar to the corresponding CAM-B3LYP/6-31G* spectra in Fig. 6.

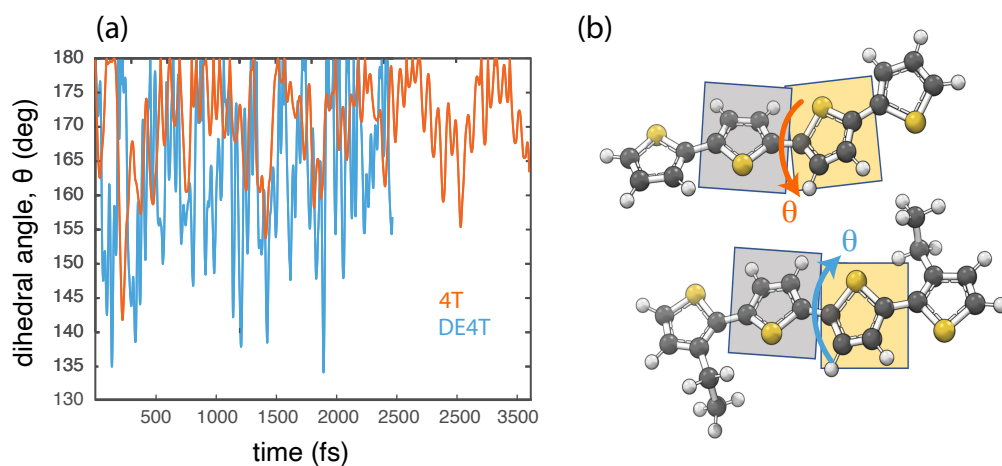


Figure S8: (a) Time evolution of the central dihedral angle θ for *ai*MD trajectories in the S_1 state of 4T and DE4T. The time step is 0.6 fs and calculations were performed using TD-DFT at the CAM-B3LYP/6-31G* level of theory. (b) Depiction of the angle in question, as in Fig. 1.